Available online at **www.joac.info**

ISSN: 2278-1862

Journal of Applicable Chemistry
2019, 8 (2): 622-633
(International Peer Reviewed Journal)

Synthesis and Characterization of NiO Nanoparticles by Electrochemical Method: Photodegradation Kinetics of Indigo Carmine Dye and Study of Antibacterial Activities of NiO Nanoparticles

H. C. Charan Kumar, R. Shilpa, V. Ravi Shankar Rai and Sannaiah Ananda*

Department of Studies in Chemistry, University of Mysore, Manasagangotri, Mysore-570 006, **INDIA**
Email: snananda@yahoo.com

Accepted on 22nd February, 2019

ABSTRACT

Nickel oxide (NIO) Nanoparticles has been synthesized by electrochemical method, which is simple and in expensive method. Nickel oxide nanoparticle had been widely used in semiconductor magnetic fields due to high surface area adsorptive. The synthesized NiO nanoparticle was used as a catalyst for the photocatalytic degradation of indigo carmine dye under various experimental conditions. The synthesized nanoparticles were characterized by UV-Visible spectroscopy, SEM-EDX and X-ray diffraction studies. The UV-Vis spectroscopy study revealed that the band gap energy of NIO nanoparticles to be 3.04V. This was calculated using Tauc plot. The structure of NIO was found to be FCC structure which was confirmed from XRD data. SEM results showed the surface morphology of the nanoparticles and the presence of Ni and O in the nanoparticle is confirmed from EDX spectrum. The photocatalytic activity of the synthesized NIO nanoparticles was investigated by the kinetics of degradation of indigo carmine dye. The photocatalytic decolorization of the dye follows first order kinetics. The antibacterial activity of these nanoparticles was investigated.

Graphical Abstract

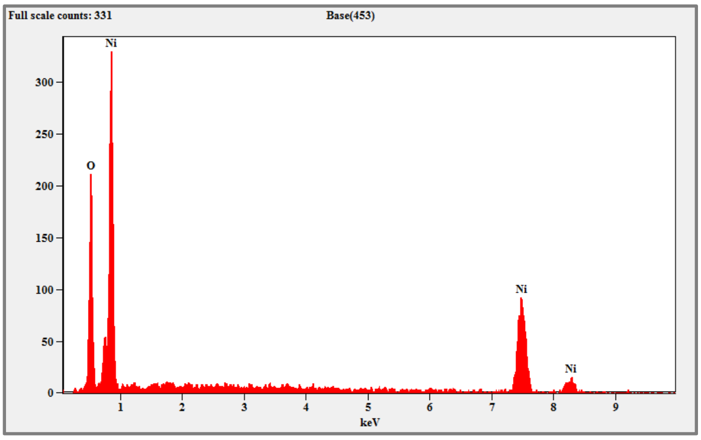

Energy dispersive X-ray analysis spectrum of NiO Nanoparticles.

Keywords: Electrochemical method, NiO nanoparticles, Indigo carmine dye, Antibacterial activity.

INTRODUCTION

In the recent years nanomaterials have much attention due to their applications like photodegradation of dyes, organic compounds and industrial effluents using metal oxide and sulphide nanoparticles and complete mineralization of organic compounds that are present as impurities in waste water. Nano structure science and technology is a broad and interdisciplinary area of research and development activity that has been growing explosively worldwide in the past few years [1-4]. Metal nanoparticles on their size and composition we can observe peculiar properties, such as quantum confinement in semiconductor nanocrystals Metal oxide nanoparticles are variety of shapes and size in nano region. Now a days the transition metal oxide nanoparticles is acting as a good nano catalyst for degradation of dyes, organic compounds and also industrial effluents [5-9]. Nickel oxide is an p-type semiconductor [10, 11].The p-type semiconductor of NiO nanoparticles becomes a interesting topic in the new area of research [12]. The NiO nanoparticles are widely used in plastics, batteries, dye sensitized solar cells and some electronic applications [13-16]. In the present manuscript we synthesized NiO nanoparticle by electrochemical method which is an environmentally friendly method by passing an electric current between two or more electrodes separated by electrolyte. The synthesized NiO nanoparticles on photodegradation of indigo carmine dye and the kinetics of degradation of indigo carmine was studied.

MATERIALS AND METHODS

All chemicals were used to prepare NiO nanoparticles were the analytical grades of purity. Ni wire was purchased from Alfa Aesar. Indigo carmine dye from lobachemie, Platinum electrode from Elico Pvt. Ltd. All solution was prepared in double distilled water. The optical properties for prepared NiO nanoparticles were studied by uv-visible spectrophotometer (shimadzu-1700 series). The X-ray crystallographic interpretations were performed by x-ray diffrometer (panalytical x-pert) using Cu Ka wavelength (λ=1.54) scanning range from 0 to 70°. The morphological feature for the prepared NiO study was determined by scanning electron microscopy (SEM-EDEX) from quanta-200 FEI, Netherlands. The elemental analysis for the conformation of prepared Ni and O is confirmed from energy dispersive X-ray analysis (EDAX).

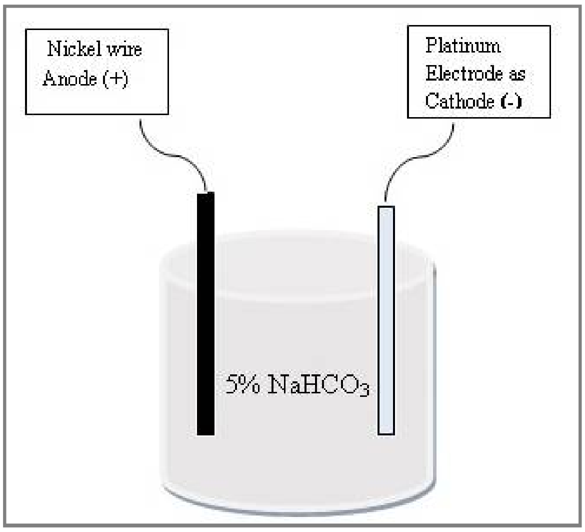

Figure 1. Experimental set up for the electrochemical synthesis of NiO nanoparticle.

Synthesis of NIO nanoparticles by electrochemical method: The nickel oxide nanoparticle is synthesized by electrochemical method. The experimental process is as shown in figure 1. The transition Ni metal wire is used as anode and platinum electrode is used as cathode. Using 20mA current and potential of 10V the experiment was run for 2 h with continues stirring. The electrolytic cell is consisting of 5 % of aqueous NaHCO3 solution. The distance of the anode and cathode during electrolysis was 2 cm. During the electrolysis the transition Ni wire starts to dissolve and give Ni ions, which are electrochemically reacted with NaHCO3 to give solid NiO. The obtained solid NiO is washed with double distilled water till complete removal of unreacted NaHCO3. The solid NiO is centrifuged and calcined for 2 h at700°C for dehydration and for the removal of hydroxides to get NiO nanoparticles. The pH of the dye solution before and after electrolysis was measured and found to be alkaline. The redox potential of Ni (-0.23).The ionic radius of Ni^{2+} are 0.72 Å respectively. Since the mechanism for the synthesized NiO nanoparticles is given in scheme 1.

$$Ni \longleftrightarrow Ni^{2+} + 2e^-$$

$$2NaHCO_3 + 2e^- \longrightarrow 2CO_2 + 2Na + 2OH^-$$

$$Ni^{2+} + 2OH \xleftrightarrow{-} Ni\,(OH^-)_2$$

$$Ni\,(OH)_2 \longleftrightarrow NiO + H_2O$$

$$\overline{\hspace{20em}}$$

$$Ni + 2NaHCO_3 \longleftrightarrow NiO + CO_2 + 2Na + H_2O$$

$$\text{In general, Metal} + NaHCO_3 \longleftrightarrow Ni + CO_2 + Na + H_2O$$

$$\text{The overall reaction } Ni + NaHCO_3 \longrightarrow \text{NiO nanoparticles}$$

Scheme 1. Synthesis of NiO nanoparticles.

Determination of photocatalytic activities: Indigo carmine (IC) dye properties, Molecular formula: C16H8O8N2S2, Molecular weight: 466.16, Λmax = 610 nm. The dye solution (2×10^{-5} M) was prepared by dissolving in distilled water. This solution was used as a test contaminant for evaluating photocatalytic activities of the prepared NiO nanoparticles. The exploration was carried out under tungsten-halogen UV-light in order to check the effectiveness of NiO nanoparticles. To check the photocatalytic activity, 20 ml of colloidal solution were transferred to centrifuge tube and centrifuged at 800 rpm to remove the dispersed catalyst and the percentage transmittance was recorded for the clear solution. The COD has been reported bothbefore degradation and after degradation of the indigo carmine dye solution using dichromate oxidation method [17, 18]. COD effect was calculated by the following equations.

$$COD = \frac{(\text{Blank} - \text{Sample}) \times N_{FAS} \times 8000}{V_{Sample}} \qquad \ldots(1)$$

RESULTS AND DISCUSSION

UV-Visible spectra: It is clear that from the optical absorption spectra. The synthesized NiO nanoparticle has showed that maximum intensity peak at 330.01 nm in the UV-region and there is no absorption peak in the visible region, Further, the rate of degradation of indigo carmine in presence of sunlight is very slow compare to UV light. The UV-Visible spectrum of NiO nanoparticles over the range 200-700 nm showed that the synthesized nanoparticles are photoactive under ultraviolet radiation. The band gap of NiO nanoparticles was calculated using Tauc plot [19] by plotting $(\alpha\ hm)^{1/2}$ verses hγ. The band gap energy could be thus estimated to be 3.04eV for NiO nanoparticles.

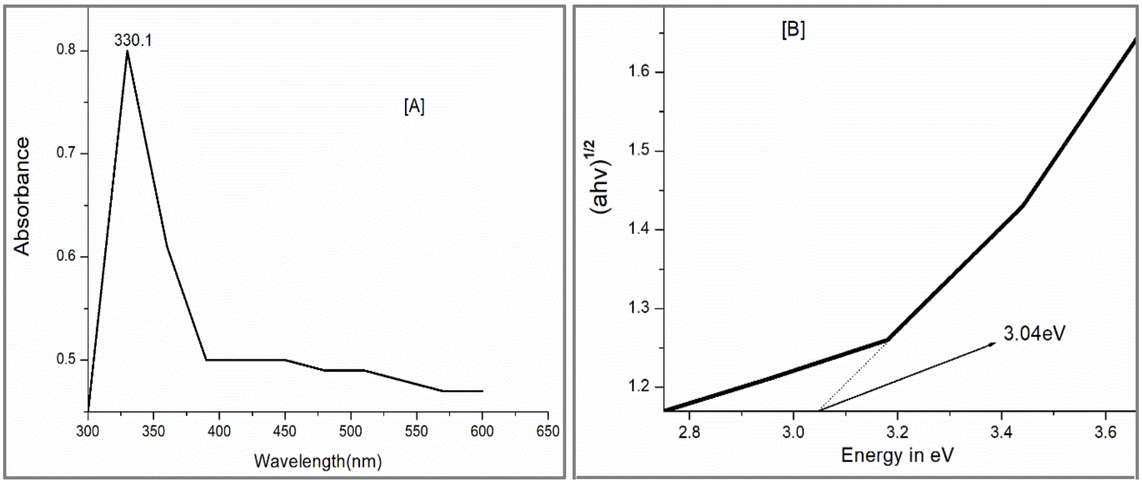

Figure 2. UV-Visible spectra (A) and Tauc plot (B) of NiO nanoparticles.

X-ray Diffraction: The purity and crystallinity of the synthesized NiO nanoparticles were examined by using powder X-ray diffraction (XRD) as shown in figure 3. The peak position appearing at 2 theta is 37.2^0, 43.2^0 can be readily indexed as (111), (200) crystal plans of the bulk NiO nanoparticle. All these diffraction peaks can be perfectly indexed to the face-centered cubic (FCC) and crystal size was found to be 21.01nm from the XRD pattern using the Debye-scherrers formula [20].

$$D = k\lambda/\beta\cos\theta \qquad \ldots(2)$$

Where k is an empirical constant equal to 0.9, λ is the wavelength of the X-ray source, β is the full width at half maximum of the diffraction peak and θ is the angular position of the peak. With reference to the JCPDS # 44-1159 standards [21]. The peak at 37.2^0 reflects (111) plane and 43.2^0 reflects (200) plane of nickel oxide. Hence XRD analysis clearly indicates the presence of nickel oxide composition.

Scanning Electron Microscopy (SEM): The surface morphology of the synthesized samples was observed by using SEM micrographs. The SEM images of NiO nanoparticles consist of agglomerated particles figure 4. Energy-dispersive X-Ray spectroscopy (EDS) images are given in figure 5. The elements which are present and their relative proportions or quantitative results can be obtained by SEM-EDS analysis.

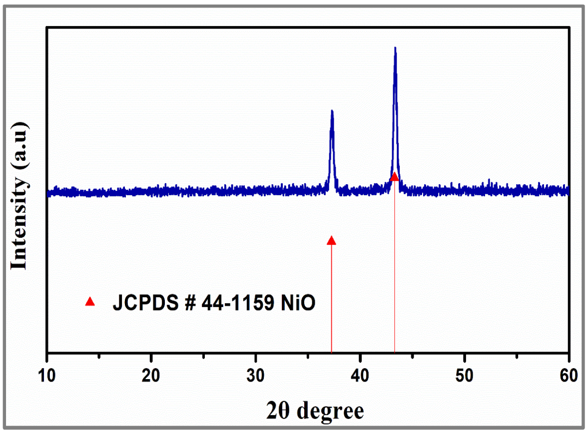

Figure 3. XRD patterns of NiO nanoparticles.

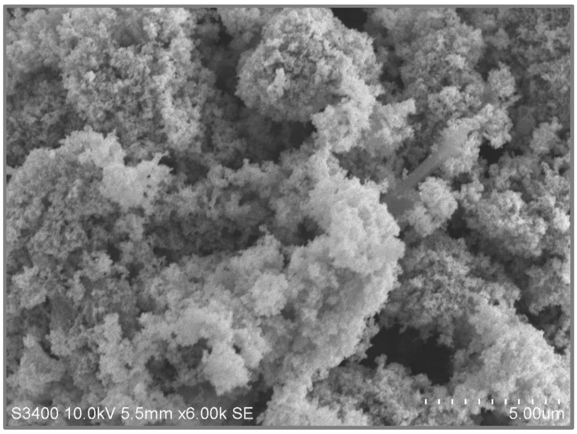

Figure 4. SEM images of electrochemically synthesized NiO Nanoparticles.

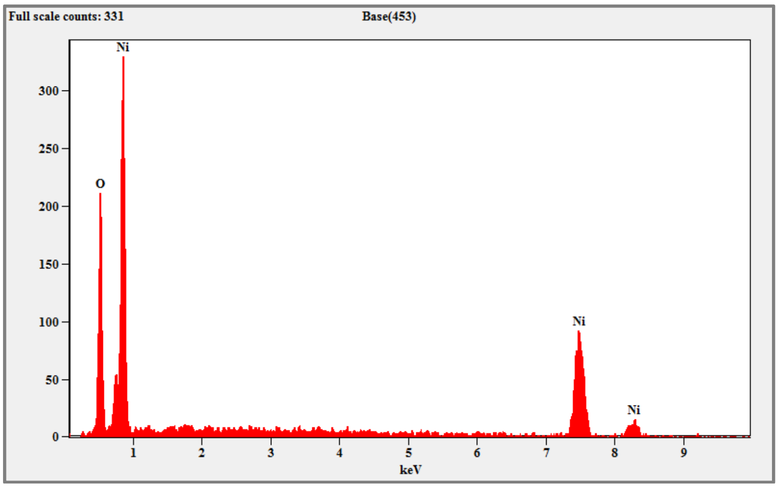

Figure 5. Energy dispersive X-ray analysis spectrum of NiO Nanoparticles.

Photodegradation Kinetics and COD Measurements

Effect of concentration of indigo carmine: The photodegradation process was performed with different concentration of indigo carmine dye solution ($1x10^{-5}$ to $5x10^{-5}$) with constant weight of nickel oxide nanoparticles as acting as a catalyst. The change in concentration of the indigo carmine was reported by change in color using spectrophotometer. A plot of log Tt (percentage transmittance of light) versus time was linear up to 60 % of the reaction indicating the disappearance of indigo carmine follows first order kinetics (Figure 6). The rate constant values are given in table 1 and the reaction rate decreased with increase in indigo carmine. The reason beyond that is with increase in the dye concentration, the solution becomes more intense colored and the path length of the photons entering the solution is decreased and the few photons reached the catalyst surface. Hence the production of hydroxyl radicals is reduced. Therefore, the Photodegradation efficiency is reduced. The COD for indigo carmine solution before and after degradation were measured and are given in table 1 and figure 7. Degradation pH before and after has been reported. It is observed that after degradation the pH of the dye solution is slightly decreased. To account for the mineralization of dye solution COD was examined at different stage. The formation of different radical species during photodegradation is given in scheme 2. The indigo carmine dye was found to have mineralized into H_2O, CO_2 and simpler inorganic salts [22, 23], after being irradiated for 5 h using NiO photo catalysts. The Photodegradation efficiency of the photo catalyst was calculated by the following formula,

$$\text{Photodegradation efficiency} = \frac{\text{Initial COD–Final COD x100}}{\text{Initial COD}}$$

$$e^-_{cb} + O_2 \longrightarrow O^-_2$$

$$h^+_{vb} + H_2O \longrightarrow H^+ + {}^{\cdot}OH$$

$${}^{\cdot}O^-_2 + H^+ \longrightarrow HO^{\cdot}_2$$

$$HO^{\cdot}_2 + e^-_{cb} + H^+ \longrightarrow H_2O_2$$

$$H_2O_2 + {}^{\cdot}O^-_2 \longrightarrow OH + {}^-OH + O_2$$

$${}^{\cdot}OH + \text{Dye} \longrightarrow CO_2 + H_2O + \text{Simple inorganic salts}$$

Scheme 2. Mechanism for the photodegradation of dye.

Table 1. Effect of Photodegradation at different concentration of indigo carmine under UV light

10^5[IC]	10^5k Sec^{-1}	Time taken for 95% Degradation in min	Effect of pH		COD Values in mg L^{-1}	
			Before degradation	After degradation	Before degradation	After degradation
1.0	9.97	60	10.13	9.19	256	16
2.0	8.44	150	9.90	9.01	352	48
3.0	7.67	220	9.76	8.80	416	32
4.0	7.29	360	9.55	8.94	512	16
5.0	5.37	520	9.32	8.61	592	48

[Nickel oxide NP] =0.02 gm 20 mL^{-1}

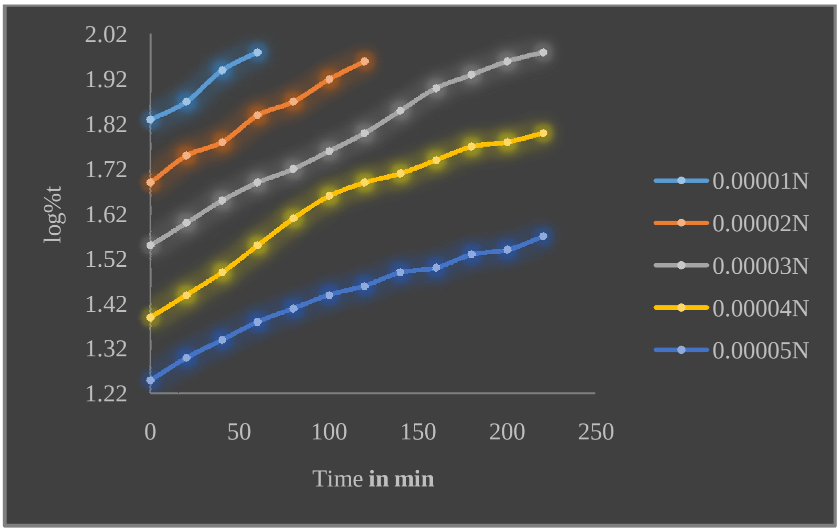

Figure 6. Effect of concentration of IC on the rate of degradation under UV light.

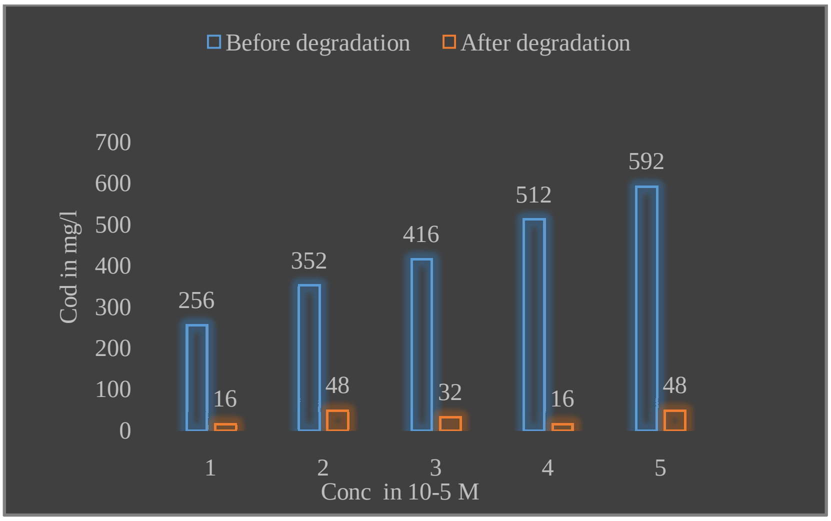

Figure 7. Effect of concentration of IC on COD values under UV light.

Effect of catalyst loading: The experiments were performed by taking different amount of catalyst varying from 0.01 to 0.04 g keeping dye concentration constant in order to study the effect of catalyst loading. The study showed that increase in catalyst loading from 0.01 to 0.04 g increased dye removal efficiency. Further increase in catalyst above 0.04 g decreased the photo activity of the catalyst, due to aggregation of NiO nanoparticles at higher concentration causing a decrease in the number of active sites on catalyst surface and increase in the light scattering of NiO nanoparticles at high concentration [24-26]. This tends to decrease the passage of light through the sample. Further, the present study indicated, from economic point of view, the optimized photocatalyst loading is 0.02 g 20 mL^{-1} (Figure 8 and Table 2). The COD effect as been reported in figure 9.

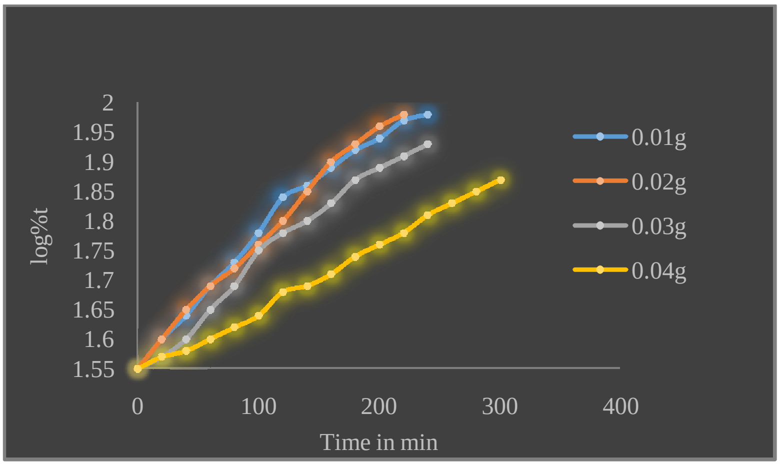

Figure 8. Effect of catalyst loading on the rate of degradation of Indigo Carmine under UV light

Table 2. Effect of catalyst loading on the photodegradation of Indigo Carmine under UV light

Catalyst NiO in mg	10^5k Sec^{-1}	Effect of pH		COD Values in mg L^{-1}	
		Before degradation	After degradation	Before degradation	After degradation
0.01	6.90	9.71	8.74	416	16
0.02	7.67	9.74	8.88	416	16
0.03	6.52	9.70	8.90	416	32
0.04	4.22	9.69	8.85	416	16

[IC]=3x10^{-5}

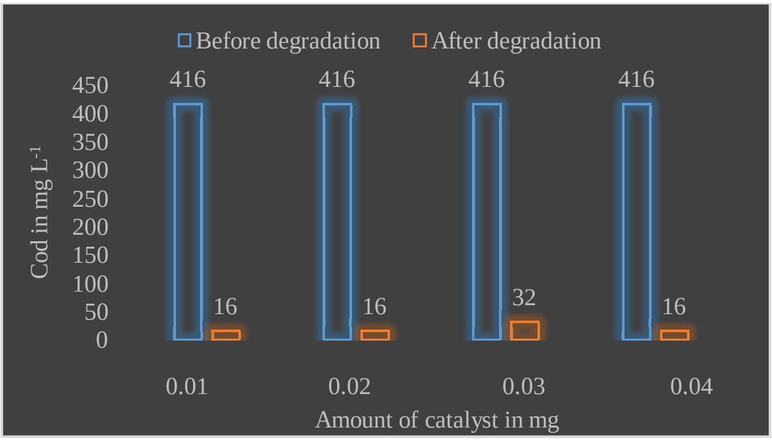

Figure 9. Effect of catalyst loading on COD values for the degradation of Indigo Carmine under UV light.

Effect of pH: The pH of the solution is one of the important factors in evaluating the Photo-degradation reaction in aqueous medium. In the present manuscript, the pH of the solution was adjusted by adding 0.01 M HCl solution and 0.01 M NaOH. The effect of pH was studied at pH 4.0, pH 6.0 and pH 9.5 by keeping all other experimental conditions constant. The results are reported in figure 10 and table 3. From the results it is observed that the rate of photodegradation increases from pH 4.0 to pH 9.5, the rate of degradation increases with increasing pH. Also, the amount of catalyst recovered after the experiment was lowered at lower pH because of the dissolution of the semiconductor oxides at very low pH values. COD effects are reported in figure 11. The optimum pH selected is 9.5 at which photodegradation is high.

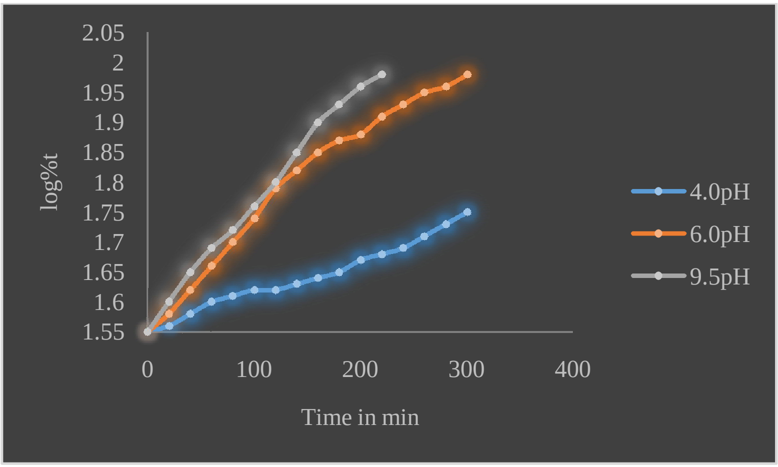

Figure 10. Effect of pH on the rate of degradation of IC.

Table 3. Effect of pH on photodegradation of Indigo Carmine under UV light

pH	10^5k Sec^{-1}	COD Values in mg L^{-1}		Photodegradation Efficiency %
		Before degradation	After degradation	
4.0	2.30	416	32	92.30
6.0	5.75	416	16	96.15
9.5	7.67	416	48	88.46

[IC dye] = 3x10^{-5} [NP] = 0.02gm 20 mL^{-1}

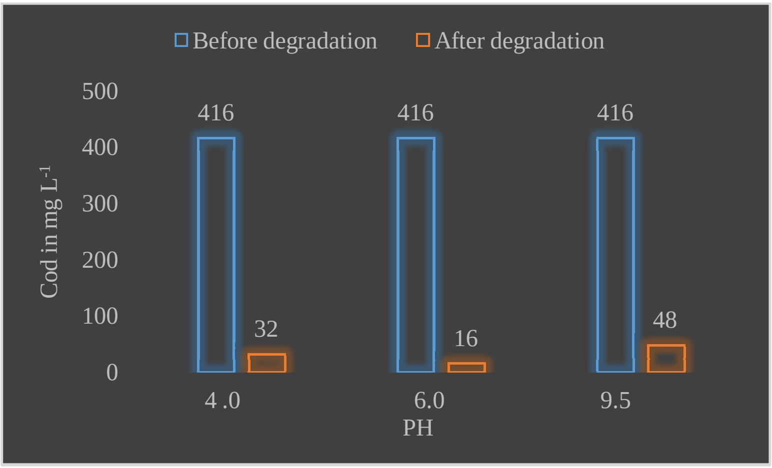

Figure 11. Effect of pH of IC on COD values.

Effect of light intensity: The photodegradation rate constant in UV light is compared with sunlight. It is perceived that the photodegradation rate constant is increased in UV light compared to sunlight for prepared nickel oxide nanoparticles. The reason beyond that is when a photon occurrence on a semiconductor(NiO) energy that overtake the band gap energy of the semiconductor .An electron is jump up from the valence band to the conduction band leaving a hole in the valence band .The excited state conduction band electrons and valence band hole can recombined and dissipate energy in the form of heat and get trapped into the metastable surface states, respectively with electrons acceptors and donors that happened to be adsorbed on the semiconductor surface .The stored energy is dissipated within a few nanoseconds by recombination in the absence of suitable e^-/h^+ scavengers .If a suitable scavenger is available to trap the electron recombination is prevented i.e. subsequent redox reaction may occur. Therefore, the nickel oxide nanoparticles act as a very good photocatalyst and is active under UV light compared to sunlight. The rate constant for degradation in sunlight and cod effects are given in table 4 and figure12.

Table 4. Effect of rate of degradation in sunlight

Catalyst 0.02g	Concentration of dye [IC] In [N]	10^5k Sec^{-1}	COD Values in mg L^{-1}		Photodegradation Efficiency %
			Before degradation	After degradation	
Nickel oxide nanoparticles	3×10^{-5}	2.68	416	48	88.46

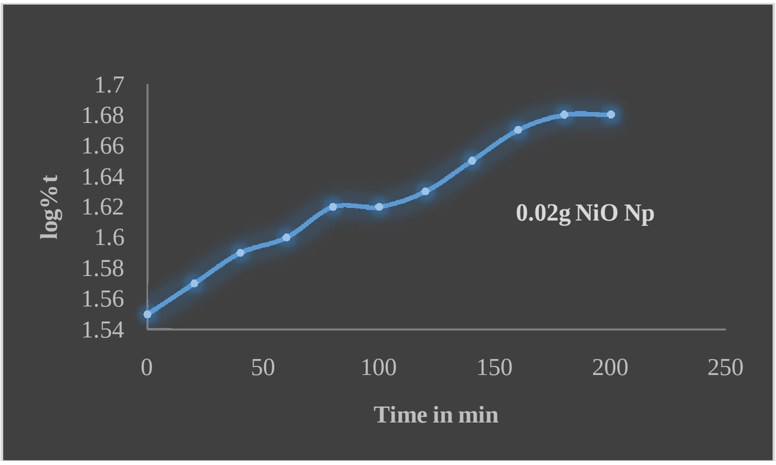

Figure 12. Effect of concentration of IC on the rate of degradation under sunlight.

Reuse of catalyst: The reuse of photocatalyst was examined to see the photodegradation efficiency of the indigo carmine dye solution. After the degradation of dye, the dye sample was kept outside without expose the UV-light for 9 h and supernatant liquid sample was decanted. The catalyst was thoroughly washed with double distilled water and reuse for the photodegradation by taking new indigo carmine dye solution. The reuse of photocatalyst shown almost same degradation efficiency compared to the fresh sample. This can be recommended the photocatalyst can be regenerated and reused.

APPLICATION

Antibacterial assay: The antibacterial susceptibility of HCC3was evaluated by using the disc diffusion *Kirby-Bauer* method in Mueller Hinton Agar Plate [27-29]. 20 mL of sterilized and molten Mueller Hinton Agar media was poured in to the sterilized Petri plates. The reference bacterial strains gram-positive *Staphylococcus aureus* (MTCC 7443) and gram-negative *Escherichia coli* (MTCC 40) obtained from Microbial Typing Culture Collection (MTCC), Chandigarh, India were cultured overnight at 37°C in Mueller Hinton Agar and adjusted to a final density of 10^7 CFU mL^{-1} by 0.5 McFarland standards. 100 µL of the pathogenic bacteria cultures were transferred onto plate and made culture lawn.HCC3 sample were loaded into 6mm sterile discs and placed on the culture plates and incubated at 37°C for 24 h. The comparative stability of discs containing *gentamycin* was made. By measuring the diameter of the ZOI formed around the disc, the antibacterial efficacy of HCC3samplewas determined.

Results: The antibacterial susceptibility of HCC3 sample was investigated by zone of inhibition by *Kirby-Bauer* disc diffusion method. Disposable plates inoculated with the Gram-positive and Gram-negative bacteria, such as *Staphylococcus aureus* and *Escherichia coli*

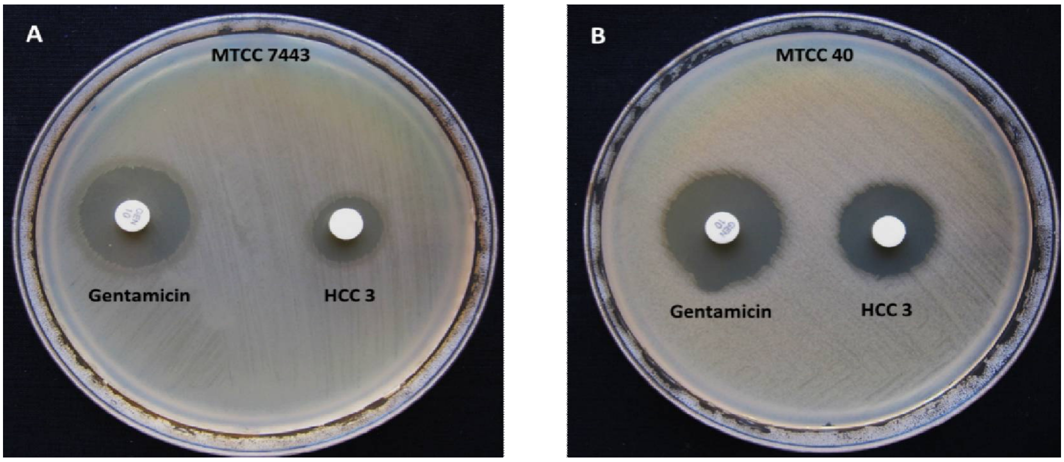

Figure 13. Appearances of inhibitory zones with (A) *Staphylococcus aureus* and (B) *Escherichia coli* bacteria.

Figure 13 shows plates to which a bacterial suspension (approximately 10^6 CFU mL^{-1}) was applied the bacteria grew to form a confluent lawn, the growth inhibition could be measured as the expansion of the clear zones surrounding the disc on the petri dish. HCC3 inhibited bacterial growth by the clear inhibition zone (a concentration of 10 µg mL^{-1}). The diameter of inhibition zones (in millimetres) around the HCC3 against test strain are shown in table 4.

Table 5. Antibacterial effect of HCC3 by Zone of Inhibition (mm) against test strains

Test Bacteria	HCC 3	Positive control *Gentamycin* (10 µg)
Staphylococcus aureus MTCC 7443	15.01 ± 0.21	32.01 ± 0.14
Escherichia coli MTCC 40	22.01 ± 0.84	30.31 ± 0.08

Note: Values are the mean ± SE of triplicate experiments

On the basis of the results obtained from microbiological studies the complex can be used as an antibacterial and antifungal agent.

CONCLUSION

In the present manuscript, the transition NiO nanoparticles are synthesized by electrochemical method an environment friendly method. The electrochemically synthesized NiO nanoparticles were characterized by SEM, EDAX, XRD, and UV analysis. The photodegradation by this semiconductor offers a green technology for removal of organic dyes present in waste water and industrial effluents. Kinetics of photodegradation of organic dye (IC) recommended that the dematerialize of IC follows 1st order kinetics. The photodegradation rate in UV light is high compared to sunlight hence the synthesized NiO nanoparticles acts as a very good photocatalyst and is active under UV light. The completeness of degradation was confirmed by COD measurement. The COD values revealed that 96% of the dye had been degraded. The synthesized nanoparticles show appreciably good inactivation of different strains of bacteria.

ACKNOWLEDGEMENTS

H.C. Charan Kumar is grateful to DST-PURSE Programme for the award of a project fellow and thanks the IOE, UPE, CPEPA, UGC-BSR and university of Mysore. R. Shilpa thanks University of Mysore for research facilities.

REFERENCES

[1]. Sowbhagya, S. Ananda, Synthesis and Characterization of Mo-Doped ZnO Nanoparticles by Electrochemical Method: Photodegradation Kinetics of Methyl Violet Dye and Study of Antibacterial Activities of Mo-Doped ZnO Nanoparticles, *International Journal of Nanomaterials and Biostructures.* ISSN 2277-3851

[2]. Mohammad Kooti, Leila Matouri, A Facile and Mild Method for Synthesis of Nickel Oxide Nanoparticles in the Presence of Various Surfactants Research and Reviews, *Journal of Material Sciences*, 37-42.

[3]. Sowbhagya, Sannaiah Anand, Synthesis and Characterization of Se-doped ZnO Nanoparticles by Electrochemical Method: Photodegradation Kinetics of Indigo Carmine Dye and Study of Antimicrobial, Antimitotic Activities of Se-doped ZnO Nanoparticles, *American Chemical Science Journal*, **2014**, 4(5), 616-637.

[4]. X. Li, X. H. Chen, G. Chen, Biosynthesis of nanoparticles by microorganisms and their applications, *J. Nanomater*, **2011**, 1-16.

[5]. K. Dhermendra, J. Tiwari, Behari, P. Sen, Time and dose dependent antimicrobial potential of Ag nanoparticles synthesized by top-down approach, *Curr. Sci*., 2008, 95, 647–655

[6]. M. L. Peterson, A. F. White, G. E. Brown, G.A. Jr Parks, Surface passivation of magnetite by reaction with aqueous Cr (VI): XAFS and TEM results, *Environmental Sci. Technol*, **1997**, 31, 1573.

[7]. P. Karpagavinayagam, C. Vedhi, Green synthesis of Novel Nickel oxide Nanoparticles using mangroves and its electrochemical characterization *International Journal of Science, Engineering and Management*, **2018**, 3(4), 699-702.

[8]. M. El-Kemaryn, N. Nagy, I. El-Mehasseb, Nickel oxide nanoparticles: Synthesis and spectral studies of interactions with glucose, *Materials Science in Semiconductor Processing*, **2013**, 16, 1747-1752.

[9]. Synthesis, characterization, applications, and challenges of iron oxide nanoparticles Nanotechnology, *Science and Applications*, **2016**, 9, 49–67.

[10]. Attarad Ali, Hira Zafar, Muhammad Zia, Ihsan ul Haq, Abdul Rehman Phull, Joham Sarfraz Ali, Hussain, D. Mohammadyani, S.A. Hosseini, S.K. SadrnezhaaD, Characterization of Nickel Oxide nanoparticles synthesized Via rapid microwave-assisted route, *International Journal of Modern Physics: Conference Series*, 2012, 5, 270–276.

[11]. M. Mohammadijooa, Z. NaderiKhorshidia, S. K. Sadrnezhaadb V. Mazinanic, Synthesis and characterization of nickel oxide nanoparticle with wide band gap energy prepared via thermochemical processing Nanoscience and Nanotechnology: An International Journal 2014; 4(1): 6-9.

[12]. M. El-Kemaryn, N. Nagy, I. El-Mehasse, Nickel oxide nanoparticles: Synthesis and spectral studies of interactions with glucose, *Materials Science in Semiconductor Processing*, 2013, 16, 1747–1752.

[13]. P.V. Chai, Muneer. M. Ba-Abbad, Y.H. Teow, A.W. Mohammad Low Temperature Condition for Nio Nanoparticles Preparation Via Sol-Gel Method. *International Journal of Advances in Science Engineering and Technology*, 2015, 3(3), 122-126.

[14]. Fardin Taghizadeh, The Study of Structural and Magnetic Properties of NiO Nanoparticles, *Optics and Photonics Journal*, **2016**, 6, 164-169

[15]. Amgad S. Danial, M. M. Saleh, S. A. Salih, M. I. Awad, On the synthesis of nickel oxide nanoparticles by sol–gel technique and its electrocatalytic oxidation of glucose, *Journal of Power Sources*, **2015**, 20, 101-108

[16]. Saeid Taghavi Fardood, Ali Ramazani, Sajjad Moradi, A Novel Green Synthesis of Nickel Oxide Nanoparticles Using Arabic Gum, *General, Industrial and Ecological Chemistry*, **2017**, 12(1), 115-118.

[17]. G. Chaitanya Lakshmi, S. Ananda, Somashekar, C. Ranganathaiah, Synthesis of ZnO/ZrO2 nanocomposites by electrochemical method and photocatalytic degradation of Fast green dye, paper dyeing and printing press effluent, *Int J Adv Mater Sci.*, **2012**, 3, 221-237.

[18]. K. Byrappa, A. K. Subramani, S. Ananda, K. M. L. Rai, R. Dinesh, M. Yoshimura, Photocatalytic degradation of rhodamine B dye using hydrothermally synthesized ZnO, *Bull Mater Sci*., **2006**, 29, 1-6.

[19]. T. P. Sharma, D. Patidar, N. S. Saxena, K. Sharma, *Indian Journal of Pure and Applied Physics*, **2006**, 44, 520-615.

[20]. B. Cullity, Elements of X-ray diffraction, *A.W.R.C inc, massachusctts*, **1967**.

[21]. Aliakbar DehnoKhalaji, Debasis Das, Synthesis and characterizations of NiO nanoparticles via solid-state thermal decomposition of nickel(II) Schiff base complexes, *Int Nano Lett*., **2014**, 4, 117 DOI 10.1007/s40089-014-0117-4.

[22]. L. Wei, C. Shifu, Z. Wei, Z. Sujuan. Titanium dioxide mediated photocatalytic degradation of methamidophos in aqueous phase, *Journal of Hazardous materials*, **2009**, 164, 154160.

[23]. Rakesh, Sannaiah Ananda, Netkal M. Made Gowda, Kithanakere Ramesh Raksha, Synthesis of Niobium Doped ZnO Nanoparticles by Electrochemical Method: Characterization, Photodegradation of Indigo Carmine Dye and Antibacterial Study, *Advances in Nanoparticles*, **2014**, 3, 133-147

[24]. N. Neelakandeswari, G. Sangami, N. Dharmaraj, Nam Ki Taek, Hak Yong Kim. Spectroscopic Investigations on the photodegradation of Toluidine Blue dye using Cadmium sulphide nanoparticles prepared by a novel Method, *Spectrochimica Acta Part A* , **2011**, 78(5), 1592-1598.

[25]. K. R. Raksha, Sannaiah Ananda, An investigation on kinetics of photocatalysis, electrical property and biological activity of electrochemically synthesized ZnS and Ru: ZnS nanophotocatalysts, *J. Applicable Chem*., **2014**, 3(1), 397-412.

[26]. K. Sudip. Batabyal, Shu En Lu, Jagadese J. Vittal, Synthesis, characterization, and photocatalytic properties of In_2S_3, $ZnIn_2S_4$, and $CdIn_2S_4$ nanocrystals, *Crystal Growth and Design*, **2016**, 16 (4), 2231-2238.

[27]. A. W. Bauer, W. M. M. Kirby, J. C. Sherris, M. Turck, Antibiotic susceptibility testing by a standardized single disk method. *American journal of clinical pathology*, **1966**, 45(4), 493-496.

[28]. Khawlah Salah Khashan, Ghassan Mohammad Sulaiman , Farah Abdul Kareem Abdul Ameer1 and Giuliana Napolitano Pak.Synthesis, characterization and antibacterial activity of colloidal NiO nanoparticles, *J. Pharm. Sci*., **2016**, 29(2), 541-546.

[29]. R.S. Raveendra, P.A. Prashanth, S. Sathyanarayani, B.M. Nagabhushana, Nio Nanoparticles and Its Antibacterial activity, *International Journal of Scientific Research and Review*, **2018**, 7(9).